On the Statistical and Fourier Modelling of Robot Motion

J. A. Tenreiro Machado, Alexandra M. S. F. Galhano

Dept. of Elec. Eng., Inst. of Eng. of Porto, Polytechnic Inst. of Porto
Rua Dr. Antonio Bernardino de Almeida, 4200-072 Porto, Portugal
tel:+351-22-8340500; fax:+351-22-8321159; e-mail:jtm@dee.isep.ipp.pt, afg@dee.isep.ipp.pt

Abstract: A new method for the study and optimization of manipulator trajectories is developed. The novel feature resides on the modelling formulation. Standard system descriptions are based on a set of differential equations which, in general, require laborious computations and may be difficult to analyze. Moreover, the derived algorithms are suited to 'deterministic' tasks, such as those appearing in a repetitive work, and are not well adapted to a 'random' operation that occurs in intelligent systems interacting with a non-structured and changing environment. These facts motivate the development of alternative models based on distinct concepts. The proposed embedding of statistics and Fourier transform gives a new perspective towards the calculation and optimization of the robot trajectories in manipulating tasks.

1 Introduction

The first step on the study of a physical system is the development of a model that usually consists on a set of differential equations. Nevertheless, many phenomena may be studied through different mathematical tools. Therefore, for a given problem, we may adopt distinct models, each with its own merits and pitfalls.

The second step on the study is the analysis of the properties revealed by the model. For a linear model we can adopt simple and clear strategies but, for a non-linear model these tools are not adequate and the analysis becomes more complex. In fact, experience demonstrates that in what concerns intelligent robotics, efficient tools capable of rendering clear results are still lacking.

The article studies a new modelling formalism based on the embedding of statistics and Fourier transform. These concepts are then illustrated on several experiments that reveal the capabilities of the new method. Bearing these facts in mind the paper is organized as follows. Section two starts by presenting the modelling formulation. Based on the new concepts, section three develops its application on the kinematic and dynamic analysis of manipulator trajectories when operating intelligently, namely for the case of random tasks. Finally, section four outlines the main conclusions.

2 Modelling Formulation

The classical kinematics of a robot having n degrees of freedom (*dof*) consists on a set of equations relating $\mathbf{p} = [p_1,\ldots,p_n]^T$ and $\mathbf{q} = [q_1,\ldots,q_n]^T$ that are the $n\times 1$ vectors of positions in the operational and joint spaces, respectively. On the other hand, the dynamics is described by a set of equations relating the joint driving torques $\mathbf{T}$ and joint positions, velocities and accelerations $\{\mathbf{q}, \dot{\mathbf{q}}, \ddot{\mathbf{q}}\}$.

Based on these equations considerable research has been done on the optimization both of the mechanical structure [1-3] and the manipulating trajectory [4-6]. However, the equations usually are non-linear and involve a plethora of variables that give rise to a cumbersome work both in the analysis and design stages. Moreover, the algorithms are suited to 'deterministic' tasks, such as those appearing in a repetitive work, and are not well adapted to a 'random' operation that occurs in intelligent systems interacting with a non-structured and changing environment.

In order to overcome the problems alternative concepts are required. Statistics is a mathematical tool well adapted to handle a large volume of data [7-8] but that is not capable of dealing with time-dependent relations. Therefore, to surpass the limitations of statistics [9-10], the new method [11-14] takes advantage of the Fourier transform by embedding both tools. In this line of thought, the first stage of the new modelling formalism starts by comprising a set of input variables that are free to change independently (*ivs*) and a set of output variables that depend on the previous ones (*ovs*).

As usually, in the direct kinematics the *ivs* and *ovs* are established by the relation $\psi:\{\mathbf{q}, \dot{\mathbf{q}}, \ddot{\mathbf{q}}\} \to \{\mathbf{p}, \dot{\mathbf{p}}, \ddot{\mathbf{p}}\}$, while for the inverse kinematics we get $\psi^{-1}:\{\mathbf{p}, \dot{\mathbf{p}}, \ddot{\mathbf{p}}\} \to \{\mathbf{q}, \dot{\mathbf{q}}, \ddot{\mathbf{q}}\}$. The inverse dynamics corresponds to the relation $\varphi:\{\mathbf{q}, \dot{\mathbf{q}}, \ddot{\mathbf{q}}\} \to \{\mathbf{T}\}$. For both cases, we can establish a set of parameters that depend on the manipulator structure and the time/space evolution of the trajectories.

The second stage of the formalism consists on the embedding of the statistical analysis into the Fourier transform through the algorithm:

i) A statistical sample is obtained by driving the manipulator through a large number of trajectories (generated with a statistics according with the task requirements) having appropriate time/space evolutions. All the *ivs* and *ovs* are calculated and sampled in the time domain.

ii) The Fourier transform is computed for each of the *ivs* and *ovs*.

iii) Statistical indices are calculated for the Fourier spectra obtained in *ii).*

iv) The values of the statistical indices calculated in *iii)* (for all the variables and for each frequency) are collected on a 'composite' frequency spectrum entitled Statistical Harmonic Content (*SHC*) of the signal.

Obviously, the previous procedure may be repeated for different numerical parameters (lengths, masses), distinct time/space trajectories and several robot structures, and the partial conclusions integrated in a broader paradigm.

3 Random Manipulating Tasks

In order to illustrate the new model, in this section we analyze the kinematics and dynamics of robots performing non-repetitive manipulating tasks. In the experiments we adopt the *RR* robot and straight lines (*SL*) or direct parabolic (*DP*) trajectories in the operational space. We consider the alternatives of a time evolution of the acceleration with On/Off (*O*) and triangular (*T*) profiles, with a maximum acceleration (A_{max}) limitation, for a total traveling time (t_{max}) and trajectory distance (*dist*), given by the expressions $t_{max} = 2(dist/A_{max})^{1/2}$ and $t_{max} = (8dist/A_{max})^{1/2}$, respectively. The results for other types of space/time kinematic trajectories and robots structures may be found in [11].

Once defined the system 'excitation' the inverse kinematics $\psi^{-1}:\{\mathbf{p},\dot{\mathbf{p}},\ddot{\mathbf{p}}\}\rightarrow\{\mathbf{q},\dot{\mathbf{q}},\ddot{\mathbf{q}}\}$ and inverse dynamics $\varphi:\{\mathbf{q},\dot{\mathbf{q}},\ddot{\mathbf{q}}\}\rightarrow\{\mathbf{T}\}$ lead to the corresponding *ovs*.

For example, Figs. 1 and 2 show the *SHCs* of the kinematics *ivs* and *ovs* for a random sample of several trajectories in the experiment {*SL, O*}. The start and end trajectory coordinates were generated randomly with a uniform distribution, describing working points in the operational space that occur in non-repetitive tasks. Fig. 3 shows the corresponding *ovs* for the dynamics.

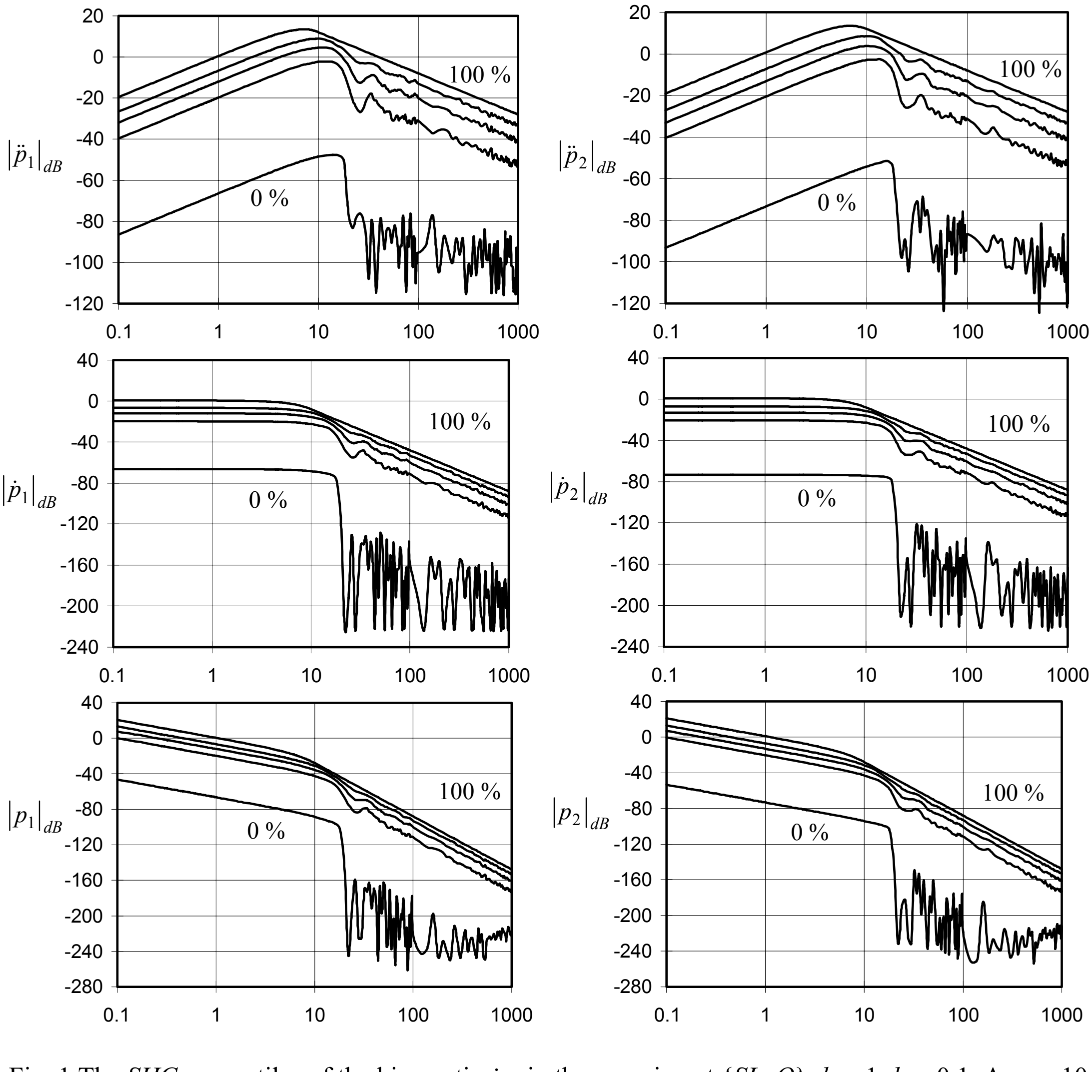

Fig. 1 The *SHC*-percentiles of the kinematic-*ivs* in the experiment {*SL*, *O*}, $l_1 = 1$, $l_2 = 0.1$, $A_{max} = 10$.

Integrating the simulation results we observe the properties:

- Numerical convergence - After repeating a large number of experiments the charts with the *SHC* of the variables do not change significantly.
- Derivative/integral sensitivity - Although being composite curves, the *SHC* still obey the 'standard' *j*ω operator for variables that are related by the derivative operator in the time domain.
- Analytical coherence - The numerical data that results from the experiments 'fits' the analytical expressions that lead to clear conclusions.
- Compatibility - The conclusions based on the analysis of the *SHC* are coherent with the results of previous studies using different mathematical tools [1,2]. For example, if $l_1 + l_2 = \text{constant}$ we verify that the maximum gain and bandwidth of the *SHC* occurs for $l_1 = l_2$.

Furthermore, the novel approach integrates, intrinsically, both the kinematics and dynamics. In fact, Fig. 3 shows that the joint torques have a *SHC* with a peak around $\omega_p \approx 10$ *rad/s*, which is due to the type of kinematic 'excitation', as can be derived from Figs. 1 and 2.

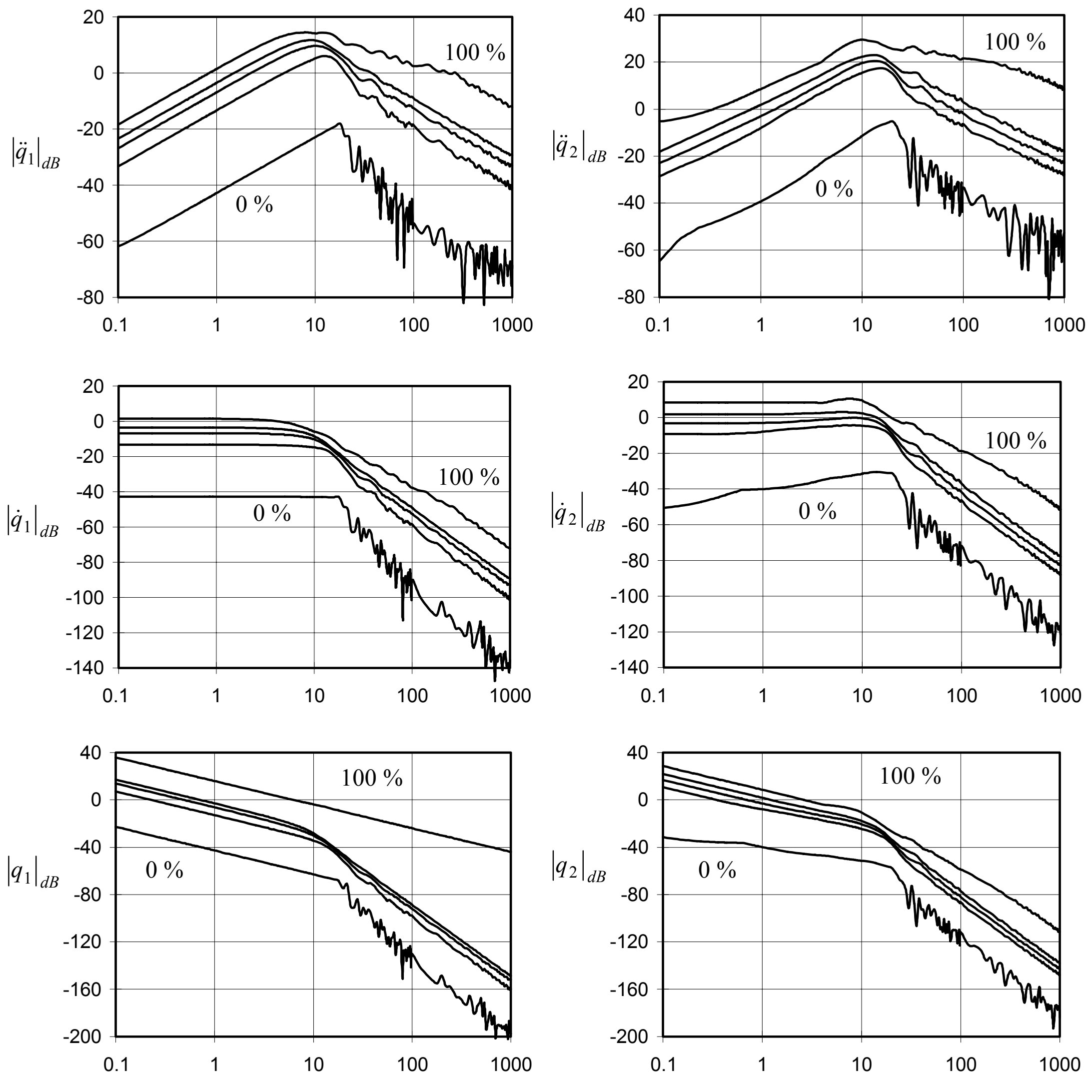

Fig. 2 The *SHC*-percentiles of the kinematic-*ovs* in the experiment {*SL*, *O*}, $l_1 = 1$, $l_2 = 0.1$, $A_{max} = 10$.

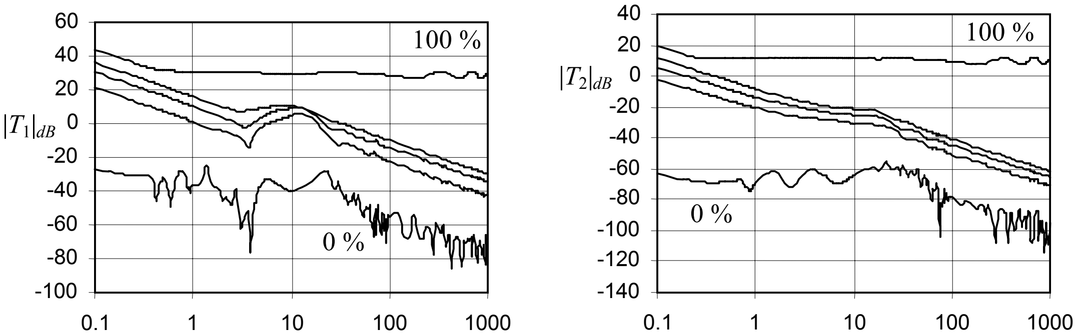

Fig. 3 The *SHC*-percentiles of the dynamic-*ovs* in the experiment {*SL*, *O*}, $l_1 = 1$, $l_2 = 0.1$, $A_{max} = 10$.

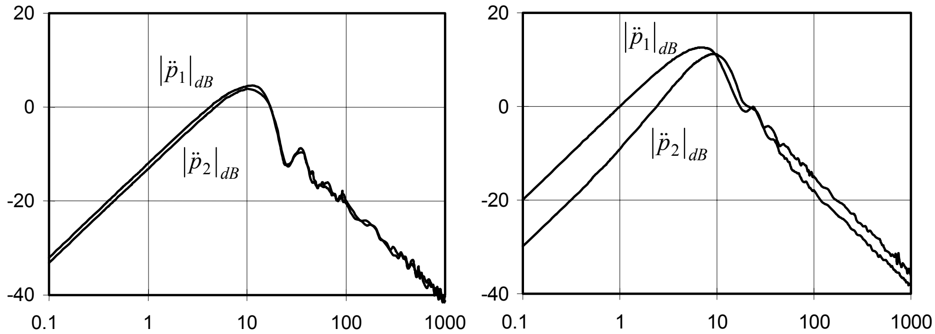

Fig. 4 The 50%-percentiles of the *SHC* of the kinematic-*ivs* in the experiments {*SL*, *O*} and {*DP*,*O*}, $l_1 = 1$, $l_2 = 0.1$, $A_{max} = 10$.

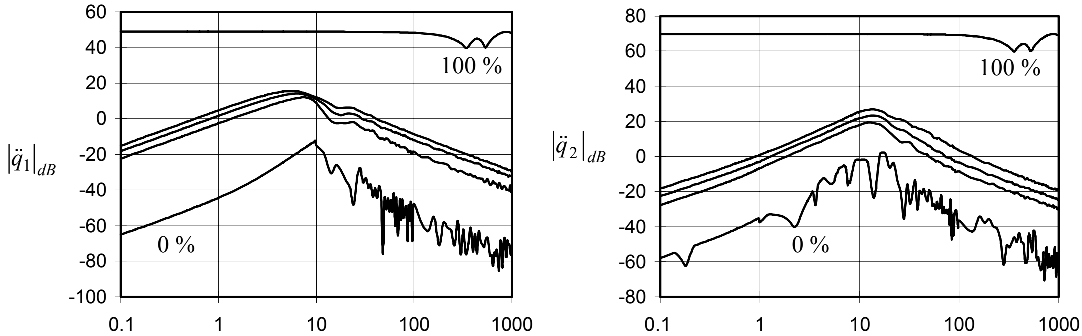

Fig. 5 The *SHC*-percentiles of the kinematic-*ovs* in the experiment {*DP*, *O*}, {*SL*, *O*}, $l_1 = 1$, $l_2 = 0.1$, $A_{max} = 10$.

The *SHC* of *ovs* depends not only of the system structure but also on the type of excitation that, for the kinematics, corresponds to the type of trajectories. In this perspective, Fig. 4 shows that the *SHC* of the *ivs* are identical for the *SL* trajectories while the symmetry is not preserved for the *DP* experiment. Moreover, the *SL* trajectories 'avoid' the singular points near the boundary of the robot workspace in contrast with the *DP* case where we may get very high amplitudes for the *ovs* as can be observed in the 100%-percentile in Fig. 5.

In what concerns the dynamics, Fig. 6 investigates the effect of adopting higher trajectory accelerations. For $A_{max} = 100$ the torque *SHC* peak moves up to $\omega_p \approx 30$ *rad/s* (*i.e.*, a factor of $10^{1/2}$) due to the influence of the inertial and Coriolis/centripetal torques ($\mathbf{T_{ic}}$). In fact, the gravitational ($\mathbf{T_g}$) and the $\mathbf{T_{ic}}$ components pose distinct requirements as revealed by Figs. 7 and 8 (for $A_{max} = 10$), respectively. As expected, the gravitational torques present low frequency requirements in contrast with the rest of the components that depend upon the velocities and accelerations.

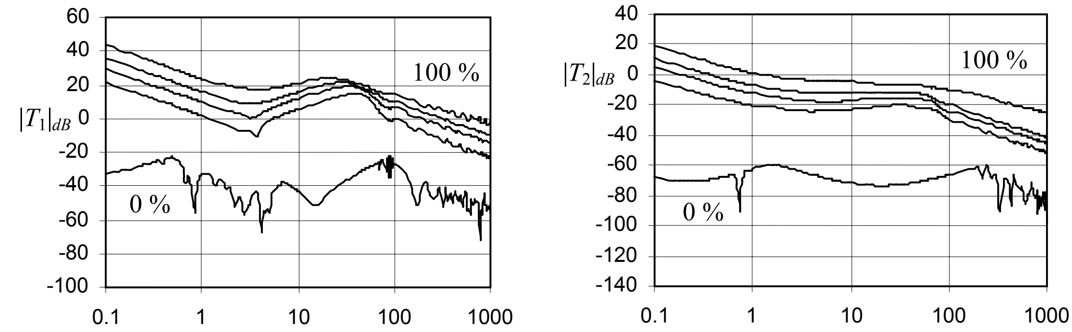

Fig. 6 The *SHC*-percentiles of the dynamic-*ovs* in the experiment {*SL*, *O*}, $l_1 = 1$, $l_2 = 0.1$, $A_{max} = 100$.

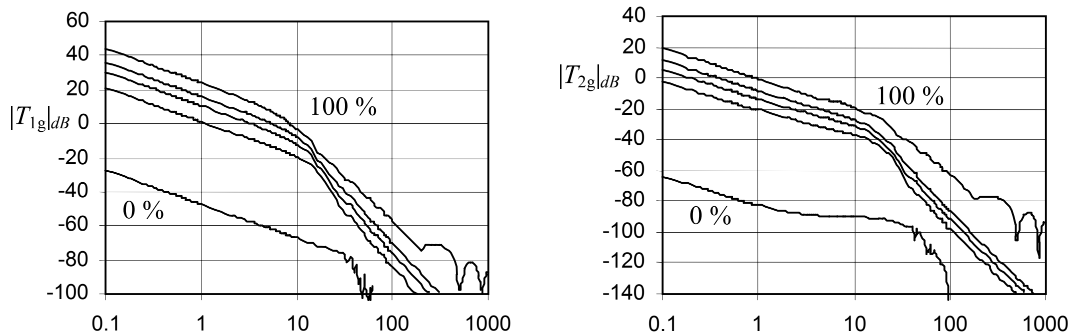

Fig. 7 The *SHC*-percentiles of the gravitational component of the dynamic-*ovs* in the experiment {*SL*, *O*}, $l_1 = 1$, $l_2 = 0.1$, $A_{max} = 10$.

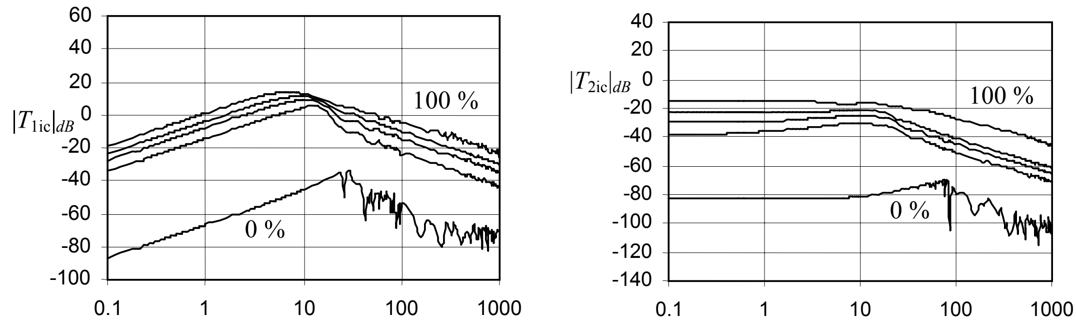

Fig. 8 The *SHC*-percentiles of the inertial plus Coriolis/centripetal component of the dynamic-*ovs* in the experiment {*SL*, *O*}, $l_1 = 1$, $l_2 = 0.1$, $A_{max} = 10$.

Finally, Fig. 9 shows the effect of using a smoother acceleration profile (*i.e.* the triangular time evolution) for a similar total traveling time. We observe that the frequency peak ω_p is maintained but, at high frequencies, the SHC passes from a decay of –20 *dB/dec* down to –40 *dB/dec* revealing the smaller actuator driving exigencies at those frequencies. Further experiments with smoother acceleration versus time evolutions confirmed this property. For example, a parabolic-like time evolution of the acceleration leads to a –60 *dB/dec* decay of the *SHC* at high frequencies. As mentioned previously, these results are not restricted to the experiments shown in Figures 1 to 9 and its dependence with the parameters and operational conditions can be evaluated heuristically [11-14]. For example, in the {*SL*, *O*} kinematics the *SHC* charts are characterized by the expressions:

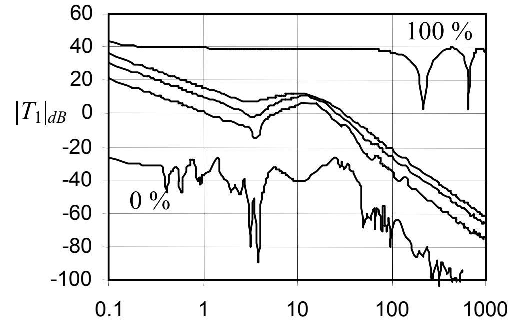

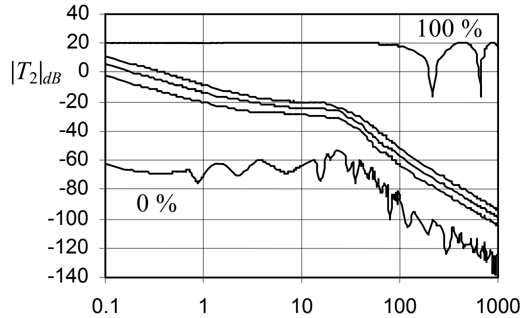

Fig. 9 The *SHC*-percentiles of the dynamic-*ovs* in the experiment {*SL*, *T*}, $l_1 = 1$, $l_2 = 0.1$, $A_{max} = 20$.

- $SHC\{\ddot{p}_1, \ddot{p}_2\}: p_{12} \sim \frac{\sqrt{A_{max}}}{\sqrt[4]{l_1 l_2}}(0.49 \pm j1.04)$, $K \sim 0.74\sqrt{l_1 l_2}$
- $SHC\{\ddot{q}_1\}: p_{12} \sim \sqrt{A_{max}}\left(\frac{0.64}{\sqrt[4]{l_1 l_2}} \pm j\frac{1.40}{\sqrt[6]{l_1^2 l_2}}\right)$,

$$K \sim \left[1.42 - 0.20\left(\frac{l_1 - l_2}{l_1 + l_2}\right) - 1.07\left|\frac{l_1 - l_2}{l_1 + l_2}\right|\right]$$

- $SHC\{\ddot{q}_2\}: p_{12} \sim \frac{\sqrt{A_{max}}}{\sqrt[4]{l_1 l_2}}(0.55 \pm j1.83)$, $K \sim 0.68$

where p_{12} are the poles and K the gain for each case.

4 Conclusions

A new method for the study of robots operating in non-repetitive manipulating tasks was presented. The novel feature consists on a non-standard approach to the modelling formalism. Usually, system descriptions are based on a set of differential equations that can be hard to tackle and are not adapted to random-like operational situations as those appearing in intelligent autonomous systems. This motivates the adoption of alternative concepts having distinct characteristics. The proposed method embeds statistics and Fourier transform and leads to clear guidelines towards the optimization of manipulator trajectories and gives a deeper insight into the requirements posed by different tasks.

References

[1] Y.C. Tsai and A.H Soni, “Accessible Region and Synthesis of Robot Arms”, *ASME J. Mech. Design*, vol. 103, pp. 803-811, Oct. 1981.

[2] T. Yoshikawa, “Manipulability of Robotic Mechanisms”, *The Int. J. Robotics Research*, vol. 4, pp. 3-9, Summer, 1985.

[3] H. Asada, “A Geometrical Representation of Manipulator Dynamics and its Application to Arm Design”, *ASME J. Dynamic Syst., Meas., Contr.*, vol. 105, pp. 131-142, 1983.

[4] G. Sahar and J.M. Hollerbach, “Planning of Minimum-Time Trajectories for Robot Arms”, *The Int. J. Robotics Research*, vol. 5, pp. 90-100, 1986.

[5] J. M. Hollerbach, “Dynamic Scaling of Manipulator Trajectories”, *ASME J. Dynamic Syst., Meas., Contr.*, vol. 106, pp. 102-106, 1984.

[6] V. Scheinman and B. Roth, “On the Optimal Selection and Placement of Manipulators”, *RoManSy’84: The Fifth CISM-IFToMM Symp.*, Udine, Italy, 1984.

[7] B. W. Mooring and T. J. Pack, “Aspects of Robot Repeatability”, *Robotica*, vol. 5, pp. 223-230, 1987.

[8] J. R. Singh, J. Rastegaar and S. Snee, “Determination of Manipulator Kinematic Characteristics: A Probabilistic Approach”, *Int. Journal of Robotics and Automation*, vol. 7, pp.161-170, no. 4, 1992.

[9] A. M. Galhano, J. M. de Carvalho and J. T. Machado, “The Statistical Study of Robot Manipulators”, *IEEE Int. Symp. on Intelligent Control*, Philadelphia, Pennsylvania, USA, 1990.

[10] J. T. Machado and A. M. Galhano, “Statistical Modelling of Robotic Manipulators”, *J. Systems Analysis-Modelling-Simulation*, vol. 12, pp. 101-123, 1993.

[11] J. T. Machado and A. M. Galhano, “A Statistical and Harmonic Model for Robot Manipulators”, *IEEE Int. Conf. on Robotics and Automation*, Albuquerque, 1997.

[12] J. T. Machado and A. M. Galhano, “Embedding Statistics and Fourier Transform Towards the Harmonic Modelling of Robot Manipulators”, *Int. Conf. on Advanced Robotics, Monterey*, USA, 1997.

[13] J. A. Tenreiro Machado and Alexandra M. S. F. Galhano, “A Statistical Perspective to the Fourier Analysis of Mechanical Manipulators”, *J. Systems Analysis-Modelling-Simulation*, vol. 33, pp. 373-384, 1998.

[14] J. A. Tenreiro Machado and Alexandra M. S. F. Galhano, “Fourier Analysis of Robot Trajectories in Random Tasks”, *IEEE International Symposium on Assembly and Task Planning*, Porto, Portugal, 1999.